AD736928

RIES 71-39

MODELING OF A PULSED CO/N_2 MOLECULAR LASER SYSTEM

George Abraham
and
Edward R. Fisher

DISTRIBUTION STATEMENT A
Approved for public release;
Distribution Unlimited

October 1971

This research was supported by the Advanced Research Projects Agency of the Department of Defense and was monitored by the U. S. Army Research Office-Durham under Grant No. DA-ARO-D-31-124-71-G82.

DDC
RECEIVED
FEB 18 1972
D

Research Institute for Engineering Sciences
and
Dept. of Chemical Engineering and Material Sciences
Wayne State University
Detroit, Michigan 48202

The views and conclusions contained in this document are those of the authors and should not be interpreted as necessarily representing the official policies, either expressed or implied, of the Advanced Research Projects Agency or the U.S. Government.

46

Reproduced by
NATIONAL TECHNICAL
INFORMATION SERVICE
Springfield, Va. 22151

UNCLASSIFIED

Security Classification

DOCUMENT CONTROL DATA - R & D

(Security classification of title, body of abstract and indexing annotation must be entered when the overall report is classified)

1. ORIGINATING ACTIVITY (Corporate author)

WAYNE STATE UNIVERSITY
RESEARCH INSTITUTE FOR ENGINEERING SCIENCES
DETROIT, MICHIGAN 48202

2a. REPORT SECURITY CLASSIFICATION

UNCLASSIFIED

2b. GROUP

3. REPORT TITLE

MODELING OF A PULSED CO/N_2 MOLECULAR LASER SYSTEM

4. DESCRIPTIVE NOTES (Type of report and inclusive dates)

Scientific Interim

5. AUTHOR(S) (First name, middle initial, last name)

GEORGE ABRAHAM AND EDWARD R FISHER

6. REPORT DATE

October 1971

7a. TOTAL NO. OF PAGES

47

7b. NO. OF REF'S

27

8a. CONTRACT OR GRANT NO.

DA-ARO-D-31-124-71-G82

b. PROJECT NO.

ARPA Order No. 675 Amdt.9

c.

d.

9a. ORIGINATOR'S REPORT NUMBER(S)

RIES 71-39

9b. OTHER REPORT NO(S) (Any other numbers that may be assigned this report)

10. DISTRIBUTION STATEMENT

Approved for public release; distribution unlimited

11. SUPPLEMENTARY NOTES

TECH, OTHER

12. SPONSORING MILITARY ACTIVITY

U.S. Army Research Office
Box CM - Duke Station
Durham, North Carolina.

13. ABSTRACT

A detailed numerical model has been developed for characterizing the important energy transfer processes operative in the CO/N_2 direct current discharge laser system. The model is based upon a rate equation formulation which includes 30 levels of both CO and N_2 and treats multi-quantum electron-molecule excitation processes, single quantum vibration-vibration exchange and vibration-translation energy transfer processes and both harmonic and overtone spontaneous emission terms. In this paper the time evolution of the CO vibrational distribution with and without N_2 is calculated and the associated small signal gain is predicted and compared to the measurements of Jeffers and Wiswall[4]. Good agreement is obtained between the predicted and measured delay times to maximum gain in a pulsed CO laser system for reasonable assumptions on the important system parameters. The variation in the predicted gains and time delays is explored for various values of the electron density and the translational and rotational temperature as a contribution toward improved experiment design in furthering the understanding of the phenomenology in the pulsed CO/N_2 laser system.

DD FORM 1 NOV 65 1473

UNCLASSIFIED

Security Classification

Table of Contents

	Page
Abstract	i
Introduction	1
Molecular Laser Model	4
Vibration-Vibration Exchange Rate Coefficients	10
Vibration-Translation Rate Coefficients	13
Spontaneous Emission Rate Coefficients	21
Small Signal Gain	23
Results	24
Discussion	40
Bibliography	43

ABSTRACT

A detailed numerical model has been developed for characterizing the important energy transfer processes operative in the CO/N_2 direct current discharge laser system. The model is based upon a rate equation formulation which includes 30 levels of both CO and N_2 and treats multi-quantum electron-molecule excitation processes, single quantum vibration-vibration exchange and vibration-translation energy transfer processes and both harmonic and overtone spontaneous emission terms. In this paper the time evolution of the CO vibrational distribution with and without N_2 is calculated and the associated small signal gain is predicted and compared to the measurements of Jeffers and Wiswall[4]. Good agreement is obtained between the predicted and measured delay times to maximum gain in a pulsed CO laser system for reasonable assumptions on the important system parameters. The variation in the predicted gains and time delays is explored for various values of the electron density and the translational and rotational temperature as a contribution toward improved experiment design in furthering the understanding of the phenomenology in the pulsed CO/N_2 laser system.

Introduction

Considerable interest is being shown in the CO laser system due to the high output powers[1,2] and the wide wavelength range[3] available. As a result of this interest, we have developed a numerical modeling code based upon a rate equation approach to characterize both the dynamic and the steady state (CW) behavior of the CO system. In this paper a description of the numerical code is presented together with preliminary results on modeling the delay times to maximum gain on various vibrational transitions in a pulsed CO laser. The predicted delay times are compared to available experimental data[4] and the dependence of the calculated values on the system parameters is explored.

The dynamic behavior of pulsed CO laser systems depends critically on the various rate processes which excite the molecular vibrational states and which subsequently produce rearrangement of this energy by vibration-vibration exchange processes. These rate processes are typically characterized by short time scales. On longer time scales, or for steady state (CW) operation, vibration-translation and spontaneous emission processes become important in determining the gain characteristics.

The molecular laser code to be discussed in this paper treats 30 vibrational levels of CO and 30 levels of an additive diatomic gas (N_2) with one inert diluent (He). All single quantum vibration-vibration exchange (VV) and vibration-translation (VT) processes are included for both CO and N_2. The particular models adopted in calculating the rate coefficients are described in the next section. Multi-quantum electron excitation processes are included based upon the cross section measurements of Schulz[5] and the calculations of Chen[6]. Spontaneous emission processes are included for

both the fundamental and the first overtone radiation from CO as taken from the calculations of Young and Eachus[7]. The values used in the code are given in the next section.

In order to compare the dynamic behavior of the CO vibrational levels with experimental measurements, small signal gain is calculated on each vibration-rotation line. In the results section of this paper we present the time behavior of the maximum small signal gain on each vibrational transition and compare these model calculations with the pulsed CO measurements of Jeffers and Wiswall[4]. The gain equations included in the code are also outlined in the following section.

The experimental measurements of Jeffers and Wiswall were obtained in a moderately high pressure - (about 30 torr of CO) room temperature-transverse discharge-pulsed-laser system. The duration of the pulse discharge was measured to be 0.6 μsec and the time delay until the peak of the maximum gain for each transition from 6 - 5 up to 11 - 10 was determined. These measurements have been successfully modeled by the numerical code presented here with reasonable assumptions on the system parameters, i.e., kinetic and rotational temperature, electron density, etc. The variation in this nominal calculation to changes in the input parameters has been studied in order to characterize the sensitivity of the gain and time delay predictions. Although the experimental measurements were obtained in CO and CO/He mixtures, we have also studied the effect of added N_2 gas on the predicted time delays and maximum gain curves. These latter results are particularly interesting in that they point out the effect of anharmonic VV processes and suggest the importance of gain measurements with different concentrations of added N_2 - keeping the other system parameters constant - in quantifying the CO pulsed laser phenomenology.

The paper is concluded with a discussion on the agreement of the model calculations with the experimental results. Suggestions are made for further experiments which will provide more definitive comparisons with the current model parameters as a means of fully understanding the physical and chemical processes which are operative in the pulsed CO laser system.

Molecular Laser Model

In quantitatively modeling the transient and CW operation of molecular laser systems, an understanding must be obtained of VV, VT, electron-molecule and inert diluent quenching processes in addition to the effects of emission processes on the energy content of the vibrational distribution. Although the current laser code does not contain stimulated emission processes, spontaneous emission terms are included as they can be a significant loss mechanism from the high lying vibrational levels of CO[8].

For a pure diatomic gas laser system such as CO, three time scales can be recognized in the relaxation process. The direct excitation of the CO vibrational levels through electron-molecular collisions occurs with the shortest time scale since the electron temperature in direct discharge laser systems is high and the coupling with vibrational levels is strong. On a longer time scale the VV processes rearrange the energy into higher vibrational levels producing at the same time partial inversion on subsequently higher and higher vibrational bands[9]. On the longest time scale, VT and radiation processes degrade the vibrational energy into thermal energy. It should be stressed that these time scales are not entirely separate as the electron excitation processes and the VV processes overlap enough to have a significant effect on the short time gain calculated from the vibrational transitions (vida infra). Also, the VV and VT processes overlap, particularly in the uppermost levels. In the presence of a second diatomic gas, additional time scales can be roughly separated due to the VV coupling between species which usually occurs on a longer time scale than the pure gas VV processes but shorter than the VT processes in either pure gas.

The total rate equation used in the current molecular laser model can be written as follows:

$$(1)\quad \frac{dn_r}{dt} = \sum_{s=r\pm1} \left\{ (P_{sr}n_s n - P_{rs}n_r n) + (P'_{sr}n_s n' - P'_{rs}n_r n') + (P''_{sr}n_s n'' - P''_{rs}n_r n'') \right\}$$

$$+ \sum_{s=r\pm1} \left\{ \sum_{\ell\pm m} \sum_{m} (P^{\ell m}_{sr}\ n_s\ n_\ell - P^{m\ell}_{rs}\ n_r n_m) \right\}$$

$$+ \sum_{s=r\pm1} \left\{ \sum_{S\pm R} \sum_{R} (Q^{SR}_{sr} n_S n'_s - Q^{RS}_{rs}\ n_r\ n'_R) \right\}$$

$$+ \sum_{s} (k_{sr}\ n_s N_e - k_{rs} n_r N_e)$$

$$+ (A_{r+1,r} n_{r+1} - A_{r,r-1} n_r) + (A_{r+2,r} n_{r+2} - A_{r,r-2} n_r)$$

in which n_r is the population of the rth vibrational leval and n is the total number density of CO; n'_r and n' are the corresponding densities of the second diatomic; n" is the number density of He; P_{sr} is the rate coefficient for the VT process

$$(2)\qquad n_s + n \longrightarrow n_r + n$$

in which vibrational energy corresponding to $E_r - E_s$, the difference between the energies of the rth and s^{th} states in CO, is transferred to or from translational energy; P^{lm}_{sr} is the rate coefficient for the VV process

(3) $$n_s + n_l \longrightarrow n_r + n_m$$

in which vibrational energy is exchanged within CO, the slight energy defect being compensated by translational energy; and P'_{sr} and Q^{SR}_{sr} are the analogous rate coefficients for the VT and VV processes involving the second diatomic, i.e.,

(4) $$n_s + n' \longrightarrow n_r + n'$$

and

(5) $$n_s + n'_S \longrightarrow n_r + n'_R ,$$

k_{sr} is the rate coefficient for excitation of CO from the sth to the rth by electrons of number density N_e; and the A coefficients are spontaneous emission rate coefficients.

In an earlier work[10,11], we concluded that in the pure gas case only single quantum vibrational transfer processes need to be considered. However, for mixtures of gases with greatly differing vibrational spacing there is a possibility that accidental resonant vibration-vibration exchange might involve a double quantum transition in one of the species. In general, for the lower vibrational levels, these processes will be slow by comparison to single quantum processes due to the form of the rate expressions[10,12] and we will restrict ourselves in this report to systems wherein only single quantum processes are important. It is important to point out, however, that for VV processes involving higher lying vibrational transitions, multiquantum processes can have larger rate coefficients than single quantum processes[13]. Due to the low density of the uppermost vibrational levels, the rates associated with these processes are usually small by comparison

to processes involving exchange with the low vibrational levels and thus, the approximation of single quantum VV exchange processes remains good for most practical model applications.

The full equation as shown in equation (1) can be somewhat simplified through the use of the detailed balance relationships, which may be written

(6)
$$P_{r,r+1} = P_{r+1,r}\, e^{-(E_{r+1} - E_r)/kT},$$

$$Q_{r,r+1} = Q_{r+1,r}\, e^{-(E_{r+1} - E_r)/kT},$$

$$p^{ml}_{rs} = P^{lm}_{sr}\, e^{-(E_s + E_l - E_r - E_m)/kT},$$

$$Q^{RS}_{rs} = Q^{SR}_{sr}\, e^{-(E_s + F_S - E_r - F_R)/kT},$$

and $$k_{rs} = k_{sr}\, e^{-(E_s - E_r)/kT},$$

where F_I represents the vibrational energy of the I-th level of N_2 above the zeroth level.

The equations as shown in (1) above including the detailed balance relationships shown in (6) and using the rate coefficients outlined in the following subsections have been numerically integrated by the Runge-Kutta-Merson method for a set of 30 levels of CO and 30 levels of N_2. This numerical technique has been used extensively for the integration of large sets of coupled non-linear ordinary differential equations such as are found when modeling coupled chemical reactions. A particular feature

of the code as taken from the work of Keneshea[14] is the use of a version of the steady state (S-S) approximation for those equations which satisfy an appropriate criterion. In a coupled set of rate equations such as occur for vibrational relaxation, the equation can be written

$$\frac{dn_r}{dt} = \sum F_r - \sum R_r \cdot n_r \tag{7}$$

where the $\sum F_r$ and $\sum R_r$ terms may be complicated functions of all the other concentrations and rate coefficients. Under conditions where the magnitudes of both $\sum F_r$ and the term $\sum R_r \cdot n_r$ are large but their difference very small, the time progress in the normal Runge-Kutta integration is very slow, i.e. the set of equations become "stiff". In the Keneshea version of the code as used here, each equation is checked to determine if it satisfies a S-S criterion, meaning the magnitude of the $\sum F_r$ term is large but the derivative dn_r/dt is small. When this criterion is satisfied the equation is iterated over the Δt time step using an algebraic algorithm as shown below.

For conditions under which $\sum F_r$ and $\sum R_r \cdot n_r$ are both large, rather than use the canonical S-S assumption

$$\frac{dn_r}{dt} = 0 \tag{8}$$

which leads to

$$n_r = \frac{\sum F_r}{\sum R_r} , \tag{9}$$

the more realistic assumption is made that the $\sum F_r$ and $\sum R_r$ terms are effectively constant over the Δt step leading to a first order ordinary differential equation. The solution is

$$(10) \qquad n_r(t+\Delta t) = \left(n_r(t) - \frac{\sum F_r}{\sum R_r}\right) e^{-\sum R \cdot \Delta t} + \frac{\sum F_r}{\sum R_r} \quad .$$

This solution is used for all equations satisfying the steady state criterion and is iterated over a Δt step together with the other equations which continue to be integrated by the Runge-Kutta-Merson technique. When an equation ceases to satisy S-S, it is automatically returned to the R-K-M subroutine for integration.

By the use of this S-S algorithm, the time step in the integration can be kept large while not sacrificing either stability or accuracy in the coupled set of equations.

Vibration-Vibration Exchange Rate Coefficients

In deriving a set of VV rate coefficients for use in the exchange processes involving pure CO collisions, use was made of the recent data of Hancock and Smith[15,16]. This data has been interpreted as involving long range forces for near resonant VV transfer while the non-resonant VV exchange processes are dominated by short range forces. In our previous calculations on VV rate processes[10,11] we have only included the effects of short range forces through a modified Rapp-Englander Golden VV model[12]. The expression used for these rate coefficients is

$$P_{sm}^{rn} = 1.508^{-12} \mu^{7/6} L^{10/3} \sigma^2 E_d^{4/3} T^{5/6} U_{rn}^2 U_{sm}^2 \cdot \left\{ \exp -1.32 (LE_d)^{2/3} \frac{\mu}{T}^{1/3} \right\} \tag{11}$$

where

μ = reduced mass in molar units

L = exponential potential parameter (Å)

σ = hard sphere diameter (Å)

T = kinetic temperature (°K)

E_d = energy defect between vibrational quanta being exchanged (cm^{-1})

and

U_{rn} = matrix element for the $r \rightarrow n$ vibrational transition

The matrix elements used are modified Harmonic Oscillator (HO) matrix elements[17] in which the actual energy spacing between vibrational units is used instead of the constant spacing assumed in the H-O model. Very close agreement has been found for these matrix elements by comparison to Morse Oscillator results[11].

The vibrational level dependence of these rate coefficients does not match the dependence as determined by Hancock and Smith due to the neglect of long range forces in the VV model as shown in equation (11). We have therefore developed an analytical expression which when applied to the above equation produces a forced fit to the experimental data at 300°K. The resulting rate coefficients for CO are shown in Figure 1 in comparison to the available experimental data. The temperature dependence of the rate coefficients is assumed to be given by equation (11), i.e., by the short range force expression.

For the CO-N_2 VV exchange rate coefficients in which the anharmonicity is considerably greater than in the pure gas, the short range force expression was directly used. This is expected to be a reasonable approximation for this collision case.

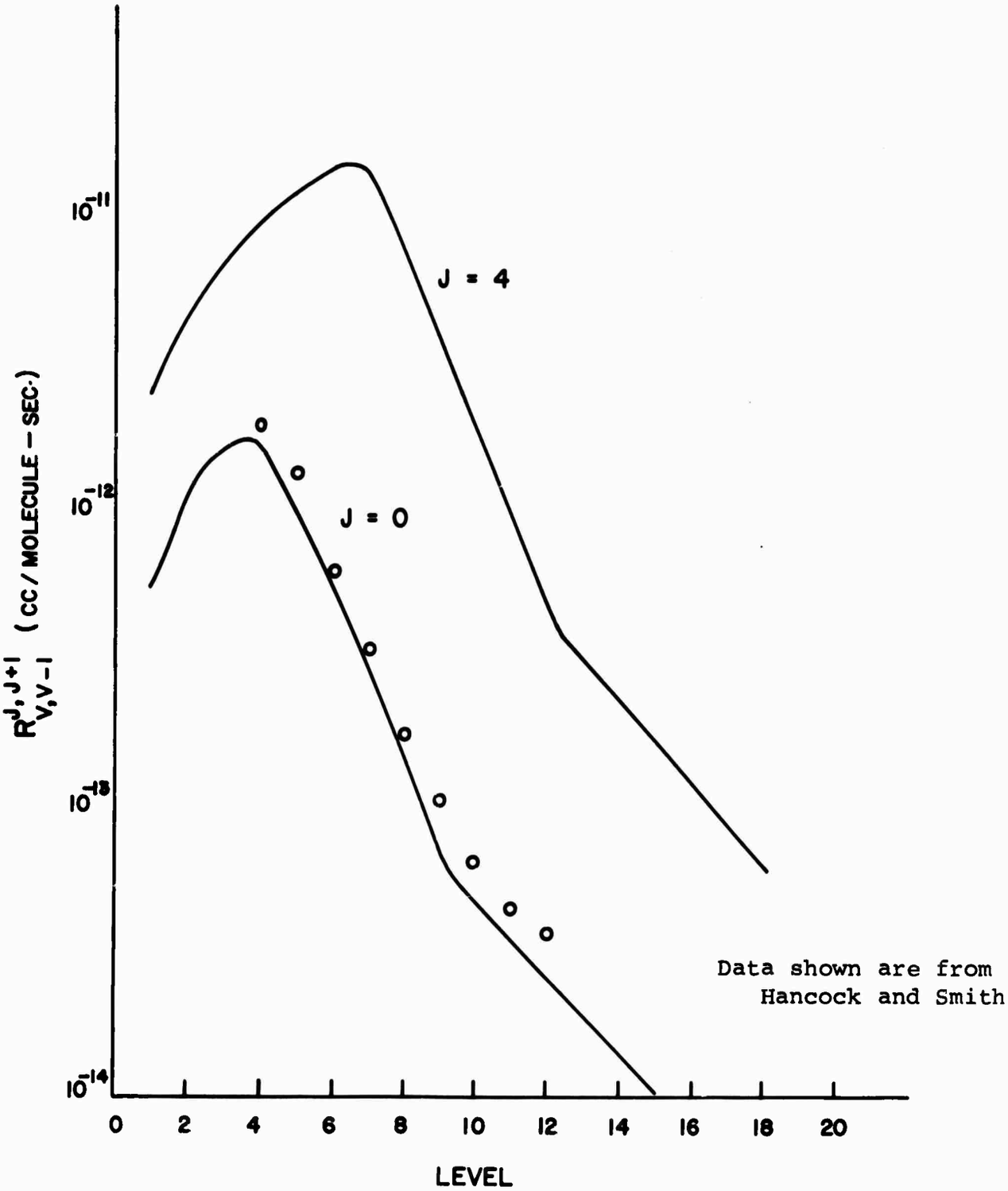

Figure 1: Vibration - Vibration Exchange Rate Coefficients for the reaction $CO(v) + CO(J) \rightleftharpoons CO(v-1) + CO(J+1)$ at 300 °K.

Vibration-Translation Rate Coefficients

Vibration-translation rate coefficients have been taken from measured relaxation times[18] using a harmonic oscillator model[19]. The expression used is

$$P_{rn} = \frac{RT}{p\tau}\left(1 - e^{-hcw/kT}\right)^{-1}\left(\frac{U_{rn}^2}{U_{01}^2}\right) \tag{12}$$

where $p\tau$ is the measured relaxation time. Scaling with vibrational level is given by the square of the vibrational matrix elements.

Electron-Molecule Rate Coefficients

The electron rate coefficients are calculated from cross section data of Schulz[5] and Chen[6]. The rate coefficients are defined in terms of the cross section, Q(V), as

$$k(T) = \int_{-\infty}^{\infty} Q(v)\ v\ f(\vec{v})\ d\vec{v} \tag{13}$$

where f(v) is the Maxwell-Boltzmann distribution of velocities. By transforming f(v)dv to a distribution of speeds, equation (13) can be written

$$k(T) = 4\pi \left(\frac{m}{2\pi kT}\right)^{3/2} \int_0^{\infty} Q(v)v^3 \exp\left\{\frac{-mv^2}{2kT}\right\} dv. \tag{14}$$

Equation (14) can be easily changed to the energy representation, yielding the following rate coefficient:

$$(15)\quad k(T) = 8\pi \left(\frac{1}{2\pi kT}\right)^{3/2} \left(\frac{1}{m}\right)^{1/2} \int_0^\infty Q(E)\ E \exp\left\{-E/kT\right\} dE$$

where $E = \frac{1}{2}mv^2$, m being the reduced mass of the collision (essentially the electron mass).

The available data on electron excitation cross sections for N_2 and CO[5,6] can be fit over a limited electron energy range $E_1 \rightarrow E_2$, where $E_2 > E_1$ by

$$(16)\qquad Q(E) = AE + B$$

where A and B are constants determined by the end point values E_1, Q_1 and E_2, Q_2.

Over the energy range $E_1 \longrightarrow E_2 = \Delta E_{12}$, equation (15) can be integrated, yielding

$$(17)\quad k(T)\Big|_{E_2}^{E_1} = 8\pi(2\pi kT)^{-3/2}(m)^{-1/2}\left[e^{-E/kT}(kT)\left\{(2kTA+B)(E+kT) + AE^2\right\}\Big|_{E_2}^{E_1}\right]$$

and

$$(18)\qquad k(T) = \sum_{\Delta E_{12}} k(T)\Big|_{E_2}^{E_1}$$

Equations (17) and (18) have been solved numerically to yield excitation rate coefficients as a function of the electron temperature using input cross section data.

The rate coefficients for the excitation of vibrational levels of N_2 and CO by electrons in the electron temperature range 1000°K to 30,000°K using the measured cross section data of Schulz[5] are shown in Figures 2 and 3, respectively. The complete numerical results for these cases are available elsewhere[20], together with the cross section data used in the calculation. In general, the error limits on the calculation rate coefficients are about ± 20%.

The spacing of the electron excitation rate coefficients for progressively larger quantum changes reflects the negative ion mechanism responsible for the excitation process. In both N_2 and CO, the negative ions are unstable by 1.89 eV[6,21] and 1.3 eV[6], respectively, corresponding to about the 6th vibrational level of each molecule. The spacing of the rate coefficients indicates a rather close coupling between levels near $v = 6$ while quantum changes greater than $\Delta v = 6$ show a considerably reduced coupling, i.e. a wider spacing.

The excitation rate coefficients calculated from the theoretical cross sections of Chen[6] are tabulated together with the corresponding cross sections elsewhere[20]. The general agreement between the calculated and measured values is within the accuracy of the overall rate coefficients, i.e. 20%.

By observing the calculated rate coefficients derived from Chen's cross sections, some indication of the scaling necessary with increasing vibrational level can be obtained. Figures 4 and 5 show this relationship for $\Delta v = 1$ and $\Delta v = 5$ processes, respectively. No trend in the calculated values are noted with increasing vibrational level in the electron temperature range between 10,000°K and 30,000°K, therefore, to within the accuracy of these calculations all excitation processes with the same Δv change can be assigned the same value as the $v = 0$ excitation case at any given electron temperature.

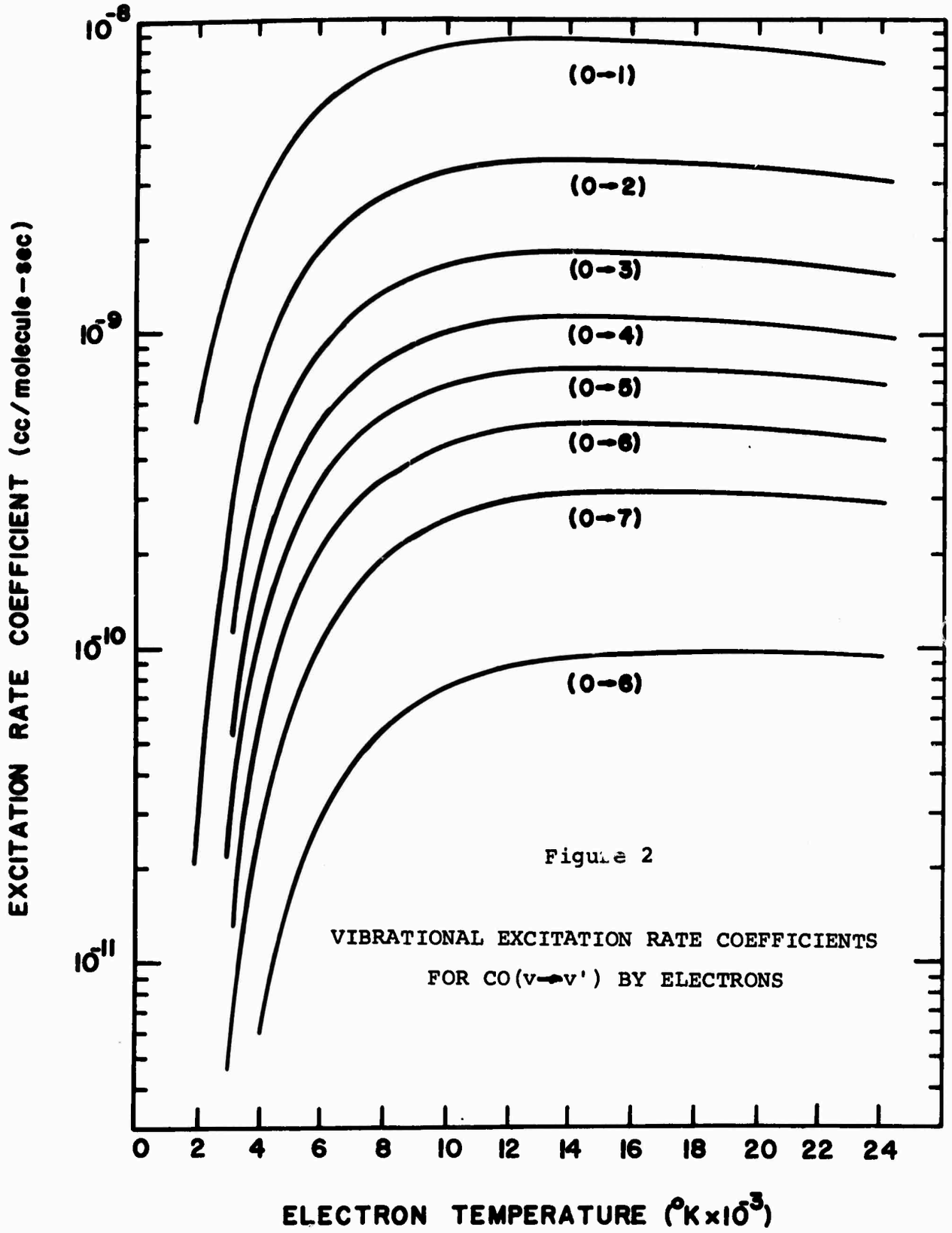

Figure 2

VIBRATIONAL EXCITATION RATE COEFFICIENTS FOR CO(v→v') BY ELECTRONS

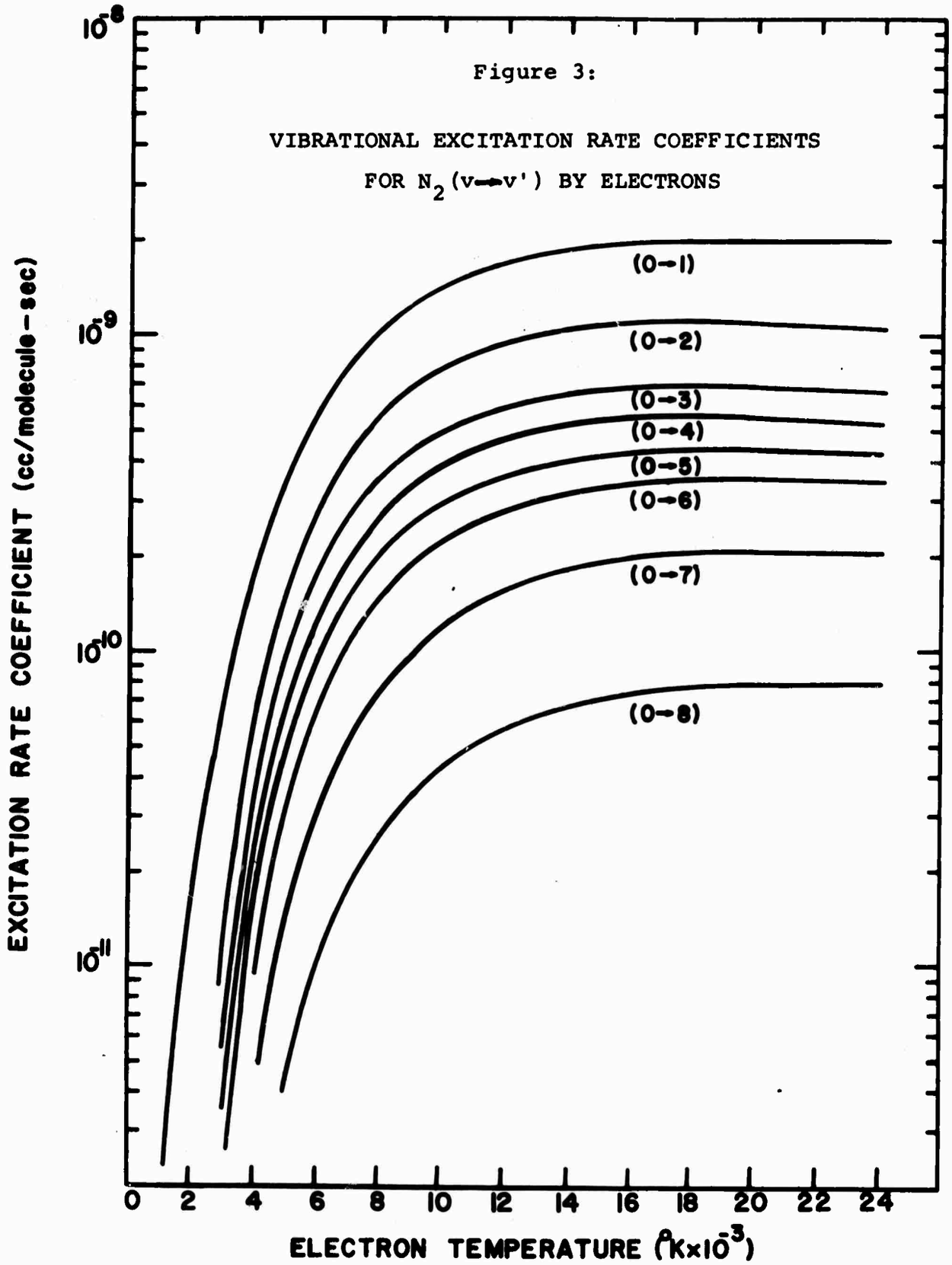
Figure 3:
VIBRATIONAL EXCITATION RATE COEFFICIENTS
FOR N_2 (v→v') BY ELECTRONS
(0→1)
(0→2)
(0→3)
(0→4)
(0→5)
(0→6)
(0→7)
(0→8)
10^{-8}
10^{-9}
10^{-10}
10^{-11}
EXCITATION RATE COEFFICIENT (cc/molecule-sec)
0 2 4 6 8 10 12 14 16 18 20 22 24
ELECTRON TEMPERATURE (°K×10^{-3})

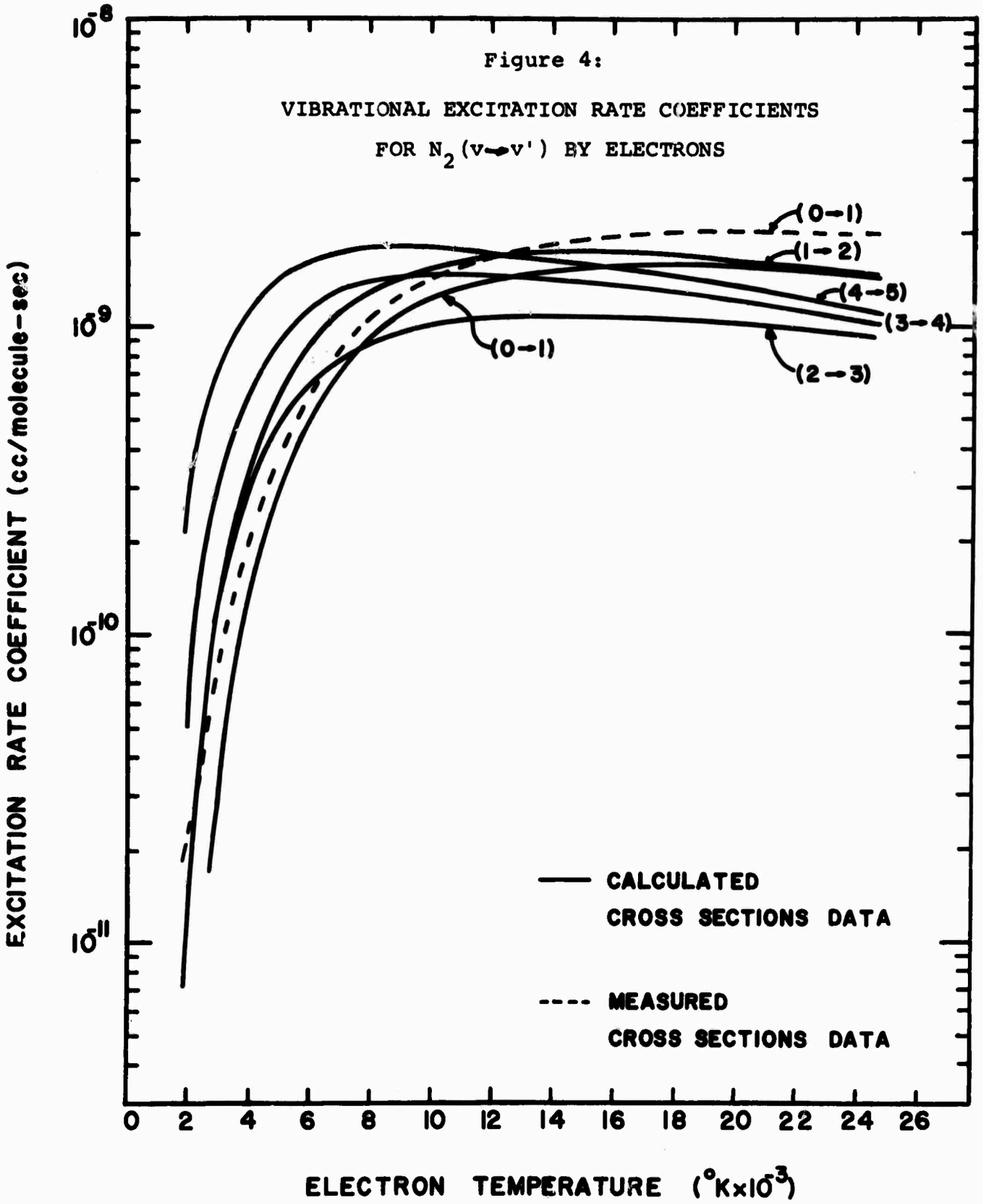
Figure 4:
VIBRATIONAL EXCITATION RATE COEFFICIENTS
FOR N_2 (v→v') BY ELECTRONS
(0→1)
(1→2)
(4→5)
(3→4)
(0→1)
(2→3)
CALCULATED
CROSS SECTIONS DATA
MEASURED
CROSS SECTIONS DATA
10^{-8}
10^{-9}
10^{-10}
10^{-11}
EXCITATION RATE COEFFICIENT (cc/molecule-sec)
0 2 4 6 8 10 12 14 16 18 20 22 24 26
ELECTRON TEMPERATURE ($^{\circ}K \times 10^{-3}$)

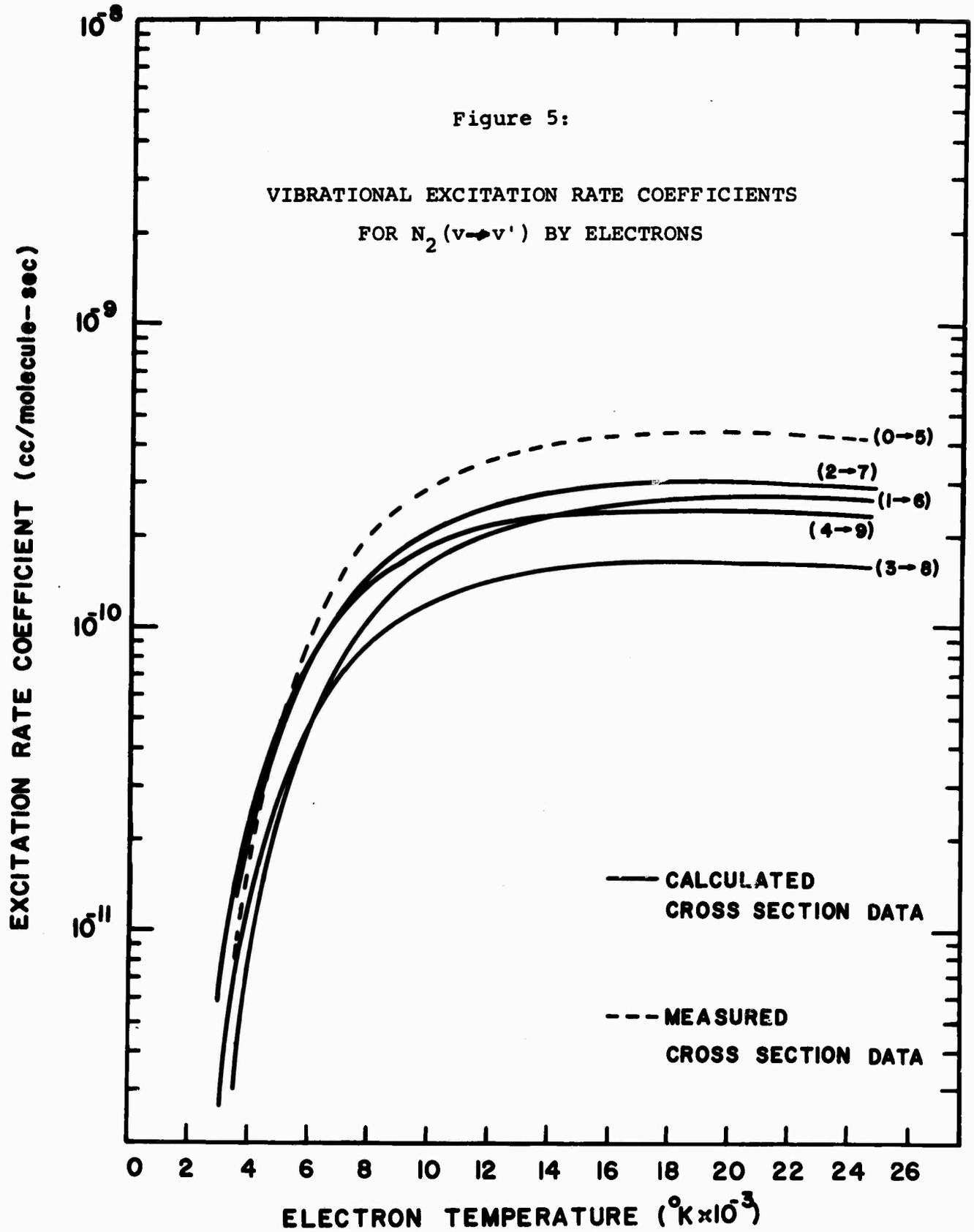
Figure 5:
VIBRATIONAL EXCITATION RATE COEFFICIENTS
FOR N_2 (v→v') BY ELECTRONS
EXCITATION RATE COEFFICIENT (cc/molecule-sec)
10^{-8}
10^{-9}
10^{-10}
10^{-11}
(0→5)
(2→7)
(1→6)
(4→9)
(3→8)
CALCULATED
CROSS SECTION DATA
MEASURED
CROSS SECTION DATA
0 2 4 6 8 10 12 14 16 18 20 22 24 26
ELECTRON TEMPERATURE ($^{o}K \times 10^{-3}$)

It is also very important to note that above about 10,000°K the electron excitation rate coefficients are effectively independent of temperature. This fact means that in calculating the vibrational distributions in a discharge environment in which the electron temperature is greater than this value, no account has to be taken of the non-Boltzmann electron distributions calculated to be present[22]. This is not the case for excitation of electronic states since these processes will be very sensitive to the high energy electron tail.

Spontaneous Emission Rate Coefficients

As part of the modeling of molecular lasers, the spontaneous emission from vibrational transitions in the infrared must be characterized. This serves two purposes; firstly, the emission from higher lying vibrational levels can be a significant energy loss mechanism in distorting the vibrational distribution and secondly, in evaluating the model laser code through side-light emission the code must be able to generate artificial spectra.

Young and Eachus[7] have evaluated 4 cubic dipole moment functions and have concluded that

$$M(r) = \pm 0.112 + 3.11(r - r_e) - 0.15(r - r_e)^2 - 2.36(r - r_e)^3 \tag{19}$$

gave the best fit to measured relative rotational line intensities in CO. Using the integrated band intensities[7] for the fundamental and overtone bands of

$$\alpha_{fundamental} = 261 \text{ amagat}^{-1}\text{cm}^{-2}$$

and

$$\alpha_{overtone} = 1.88 \text{ amagat}^{-1} \text{ cm}^{-2} ,$$

the following table of Einstein Coefficients has been generated and incorporated into the laser model code. Current work is concentrated on a subroutine to generate the entire artificial spectrum in the vibration-rotation bands including an appropriate slit function.

Table 1.

Relative Einstein Coefficients for Spontaneous Emission for CO

upper vibrational level	fundamental	overtone
1	1.00	----
2	1.93	1.00
3	2.78	3.00
4	3.53	5.96
5	4.21	9.89
6	4.81	14.74
7	5.35	20.48
8	5.74	27.03
9	6.23	34.36
10	6.58	42.43
11	6.88	51.17
12	7.14	60.54
13	7.35	70.79
14	7.60	81.62
15	7.73	92.99
16	7.83	104.82
17	7.90	117.05
18	7.93	131.84
19	7.94	147.24
20	7.83	160.27
21	7.69	173.80
22	7.53	187.53
23	7.35	201.19
24	7.16	214.94
25	7.00	228.60
26	6.74	242.13
27	6.51	255.45
28	6.27	268.52
29	5.82	281.40

Small Signal Gain

In order to model the behavior of pulsed and CW laser operation we have developed a numerical routine to calculate the gain associated with a particular vibration-rotation line. The equation for small signal gain can be found in several references[23,24] to be

$$(20) \qquad g(cm^{-1}) = \frac{4\pi^2}{3}\left(\frac{e^2}{\hbar c}\right)|R_{vv'}|^2 S_J\left(\frac{hcB}{kT}\right) N_{v'}\left(\frac{mc^2}{2\pi kT}\right)^{\frac{1}{2}}$$

$$\cdot\left[\frac{N_v}{N_{v'}}\, e^{-F_v(J \pm 1)\frac{he}{kT}} - e^{-F_{v'}(J)\frac{he}{kT}}\right]$$

where $N_{v'}$ and N_v are the vibrational populations of the lower and upper levels respectively, $S_J = J + 1$ for p branch transitions, $S_J = J$ for R branch transitions (J is the rotational quantum number of the upper level), F(J) is the energy of the Jth rotational level and is approximated by $BJ(J + 1)$, and $R_{vv'}{}^2$ is the vibrational matrix element for the transition v to v'.

Since the current application for the pulsed laser code is to systems characterized by rotational temperatures, we can either calculate the gain associated with any particular laser line, i.e. select both a v and J, or we can calculate the J value for maximum gain and thus, generate the maximum gain associated with a given vibrational transition. The results as shown in the next section represent the maximum gain on each vibrational band.

Results

The laser code outlined above has been applied to the pulsed CO laser experiments of Jeffers and Wiswall[4]. These experiments were performed at roughly 30 torr on room temperature CO with electron pulse times of about 0.6 μsec. The laser code was thus applied to an ambient CO vibrational distribution assuming various square wave pulse shape electron concentrations. Model calculations were made with time dependent kinetic and rotational temperature in which the time dependent kinetic temperature produces time dependent rate coefficients for the VV and VT processes while the time varying rotational temperature enters directly into the gain calculations. The closest agreement with the experimental results was obtained assuming that the electron density was 10^{13} electrons/cc, the kinetic and rotational temperatures being constant at T = 300°K, and with an electron pulse width of 0.6 μsec. The results of these calculations are displayed in Figures 6 through 9.

Figure 6 shows the time evolution of the initial ambient vibrational distribution of CO due to 10^{13} electrons/cc with a Maxwellian distribution at 20,000°K. As indicated in the previous section on electron excitation rate coefficients, the electrons tend to preferentially excite vibrational levels from v = 4 to v = 8 due to the negative ion excitation mechanism. This behavior is clearly indicated in the figure. At longer times, the preferential excitation is smoothed out by excitation to higher lying levels and by VV processes which become significant for times of the order of the pulse duration. The affect on the vibrational distribution due to the electron pulse of VV processes, electron concentration, and pulse width is given in Figure 7.

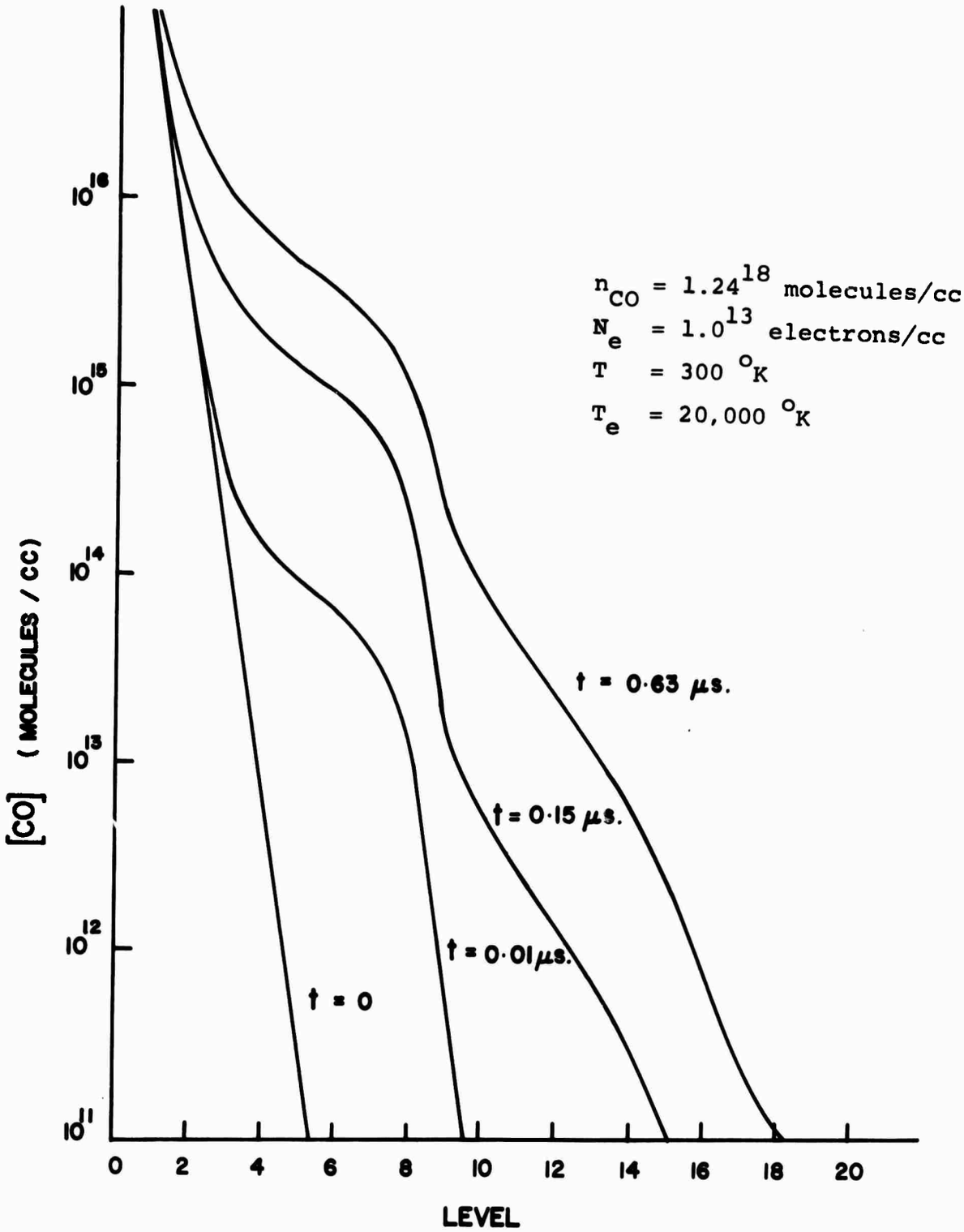

Figure 6: Evolution of the CO vibrational distribution due to hot electrons in a pulsed CO laser.

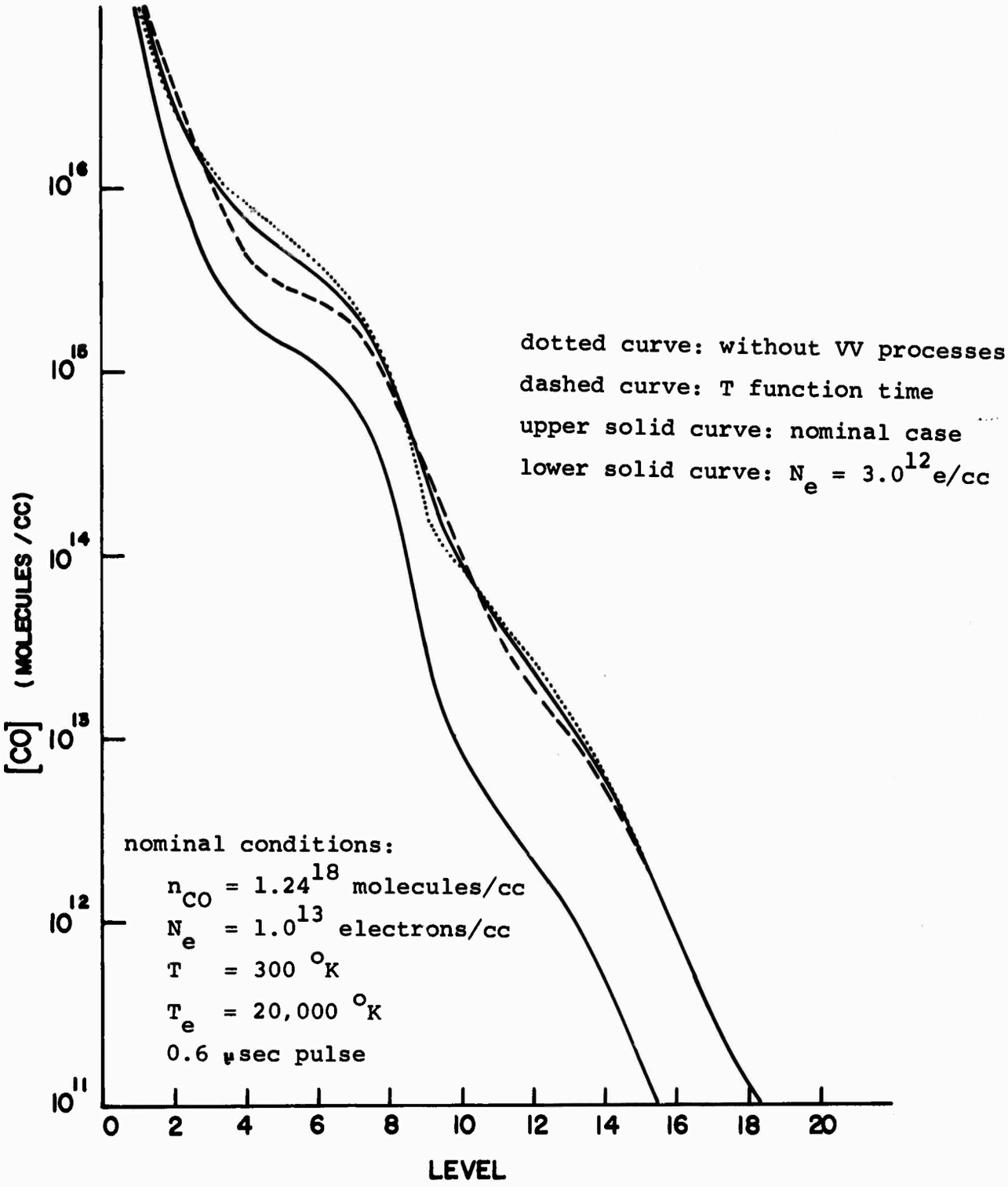

Figure 7: Final CO vibrational distribution due to 0.6 μsec electron pulse for various conditions.

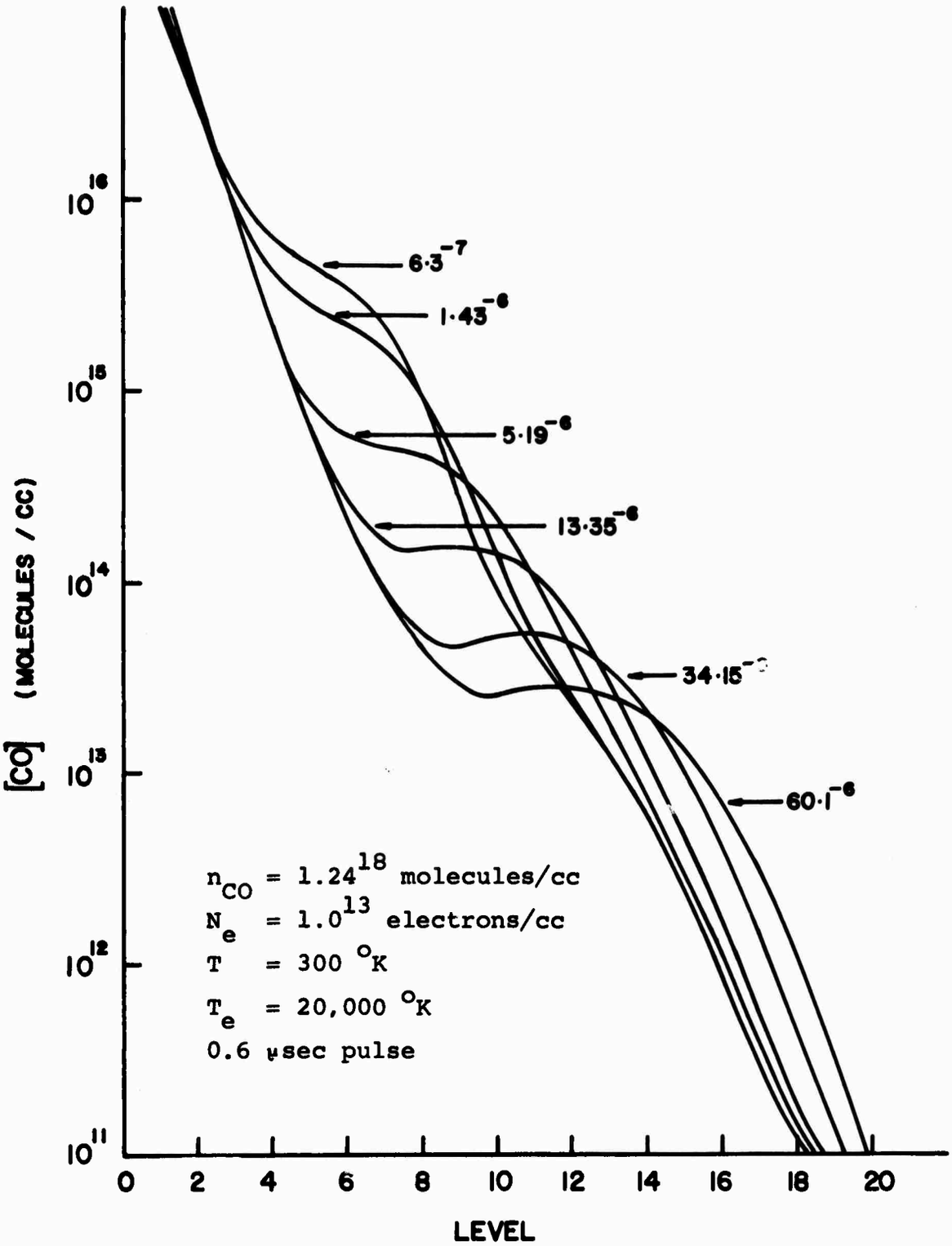

Figure 8: Evolution of the CO vibrational distribution due to VV processes following a 0.6 μsec pulse for a pulsed CO laser.

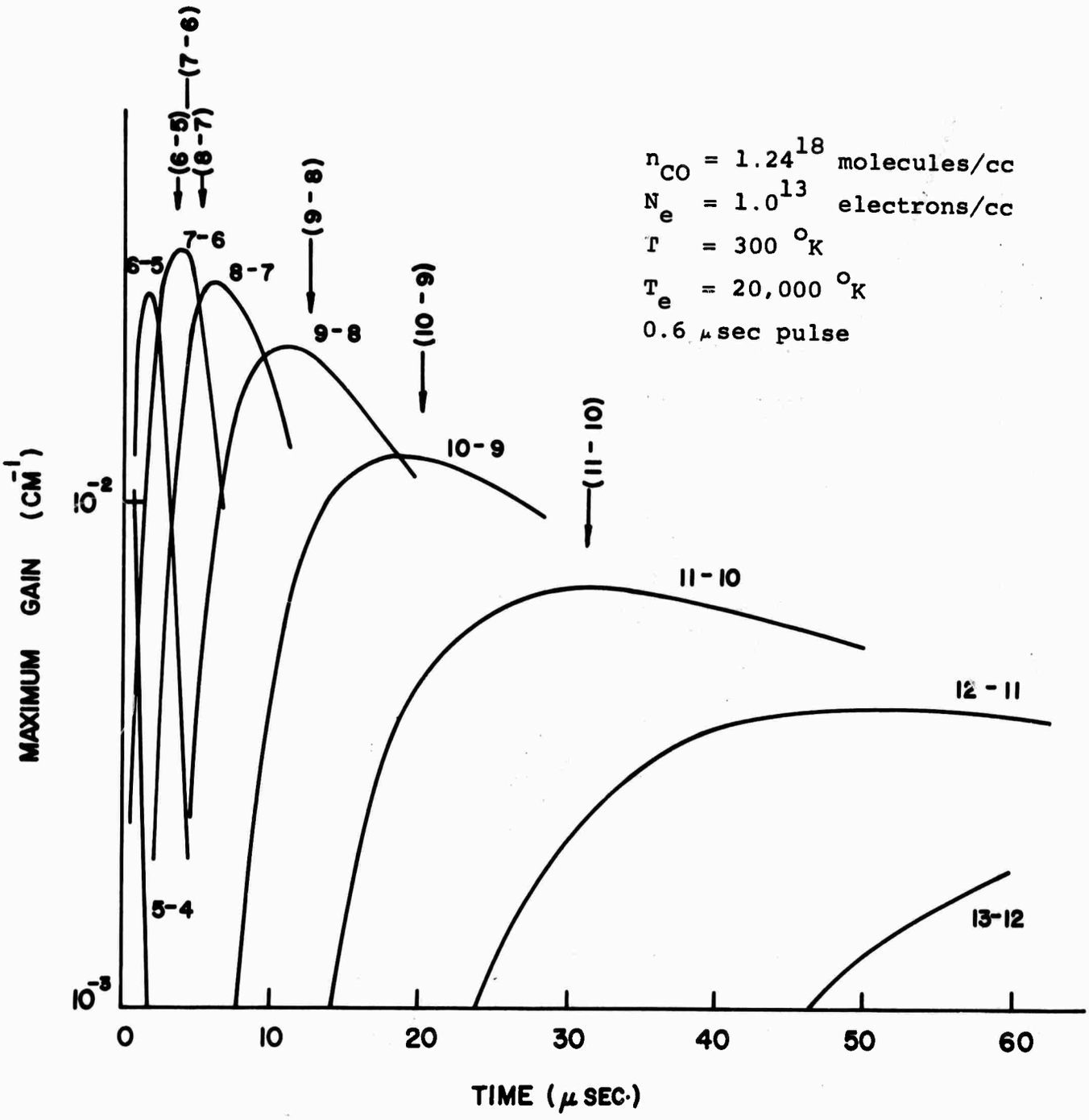

Figure 9: Time sequence of maximum gain for the fundamental transitions in a pulsed CO laser. Arrows represent data of Jeffers and Wiswall.

Without VV processes, as shown in Figure 7, the vibrational distribution is smoother, i.e. less structured, than with VV processes due to the redistribution of energy from low vibrational levels to higher levels as a result of the anharmonicity in the vibrational spacing. As the kinetic temperature is changed initially from 500°K to 300°K with a time constant of 2 μsec, the redistribution of vibrational energy is further enhanced and the vibrational distribution becomes nearly inverted between levels v = 5 and v = 7. When the electron density is reduced the energy supplied into the CO distribution is decreased as is clearly shown in the figure. The effect of these variations on the subsequent maximum gain predictions is shown in the later figures of this section.

Following the electron pulse, the vibrational distribution is redistributed entirely due to VV processes. The evolution in the vibrational distribution of CO is thus determined as shown in Figure 8. Clearly, energy flows up the vibrational structure as expected from anharmonicity arguments, however, due to the preferential excitation by electrons, vibrational energy also flows into the v = 1 level from levels between about v = 4 to v = 8. This "reverse" flow of vibrational energy tends to reduce the possibility of obtaining laser action in the low vibrational levels on time scales greater than the pulse length without the presence of an additive gas which would preferentially reduce the excitation in these low levels. This point is discussed further in the discussion section.

As shown in Figure 8, inversion is predicted to move up the vibrational structure creating a favorable condition for laser gain on higher vibrational transitions with increasing time, as has been experimentally observed[4,25,26]. The actual maximum gain predicted from this "nominal" case is presented

in Figure 9 where the measured time delays of Jeffers and Wiswall are indicated by arrows. The agreement with the time delays to maximum gain for the 7-6, 9-8, 10-9 and 11-10 transitions are very good but the 6-5 transition is predicted to be about 1 μsec sooner than observed and the 8-7 transition is predicted to be about 1 μsec later than observed. Both of these transitions are very sensitive to the electron excitation rate coefficients since they are predicted to reach maximum gain only a few μsec after the end of the electron pulse. We have not yet tried to vary the electron rate coefficients to improve the short time scale predictions since the agreement at the longer time scales is good. In the following figures the variation in these "nominal" gain predictions are studied for several different values of the important system variables. Each subsequent figure has as reference points the delay time and maximum gain associated with the "nominal" predictions together with arrows indicating the extent of variation from these "nominal" predictions.

Figure 10 shows the greatly decreased gains predicted when the electron density is reduced to 3×10^{12} electrons/cc while keeping the other system parameters constant. The results for this calculation are as expected; since the electron density is lower the energy input into the CO vibrational levels is lower and the maximum gain is lower (see equation 20). In addition, since the population of the vibrational levels is lower, the rate at which energy is redistributed due to VV processes is slower than the "nominal" case and the delay times are thus longer. Note the significant effect of a lower electron density on the maximum gain predicted from the upper vibrational transitions.

Since Jeffers and Wiswall indicated that the kinetic and rotational temperature in their pulsed experiments were increased due to energy supplied by the electron pulse, we altered the code to permit use of a time varying kinetic and rotational

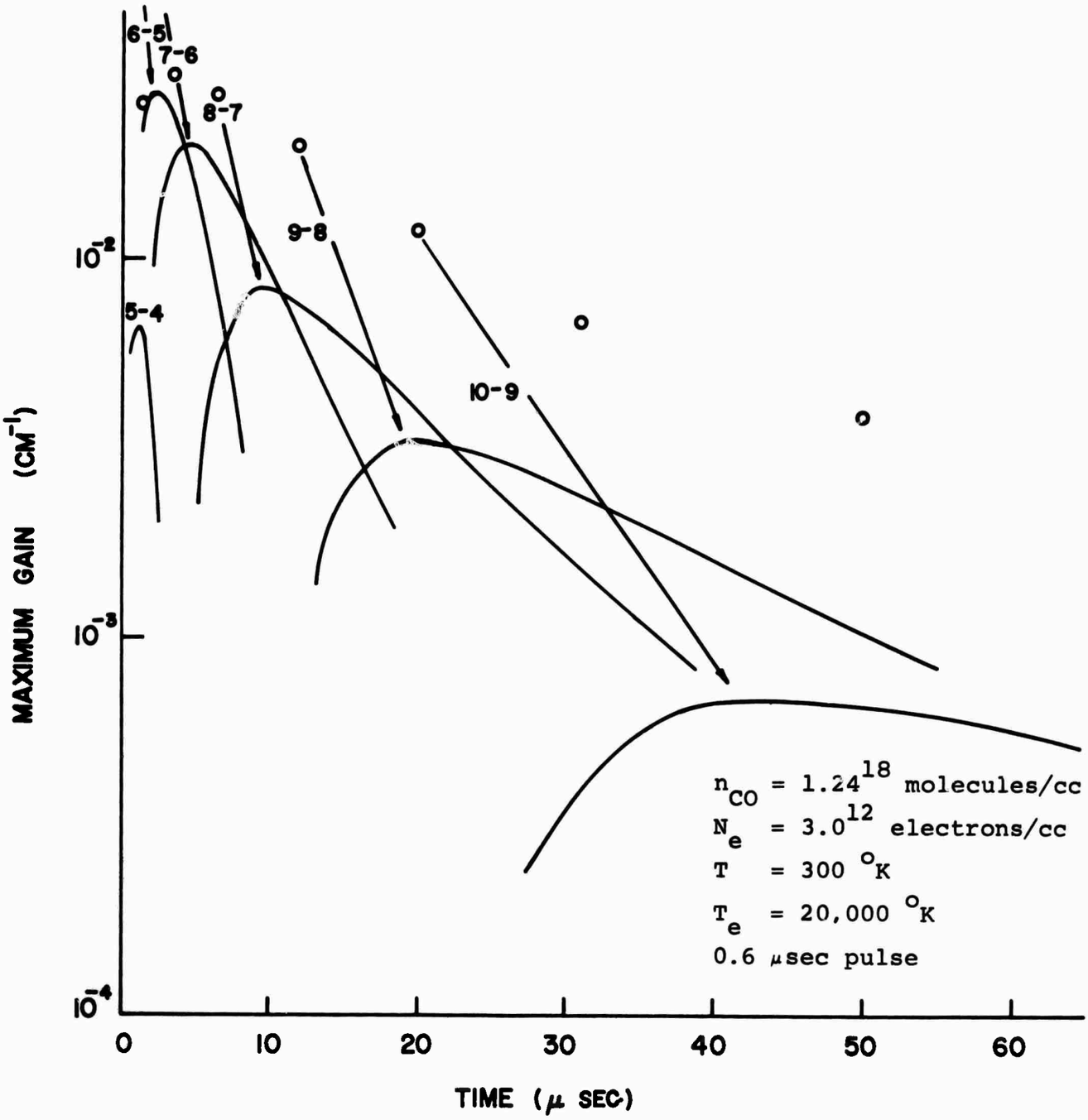

Figure 10: Time sequence of maximum gain for the fundamental transitions in a pulsed CO laser. The points refer to "nominal" pulsed CO laser predictions.

temperature having a time constant of 2 μsec. This time constant appears to be consistant with the experimental observations although quantitative results on this effect still need to be obtained. We have arbitrarily assumed that the temperature function goes from 500°K to 300°K but there is no concrete evidence to support this particular assumption. Two features of the calculation as displayed in Figure 11 are important to note; first that the time delays are uniformly shortened and that the maximum gain is decreased over the "nominal" case. The fact that the time delays are shortened is a result of the increased VV rate coefficients at the higher kinetic temperatures while the decreased gains are a result of the increased temperature on both the gain calculation and the VV processes. At higher kinetic temperatures, the exothermicity involved in transferring the larger (and lower) vibrational quanta into the smaller (and higher) vibrational levels is reduced[10]. This produces less of a tendency toward vibrational inversion and reduces the expected gain. In addition, since the rotational temperature is also higher, the gain is directly reduced by spreading out the vibrational population over more J states with a subsequent reduction in gain.

To test the sensitivity of the predicted gain characteristics and time delays to the electron pulse width, we increased the "nominal" pulse width from 0.6 μsec to 0.8 μsec while keeping the other parameters constant. The resulting maximum gain curves are shown in Figure 12. The time delays are uniformly shortened and the gains for low levels are decreased while for higher transitions the gains are increased. The decreased time delays are a result of the increased vibrational populations and subsequent increased VV rates. The gain results for low levels are a result of producing a smaller inversion due to the increased effect of electrons (being present for 0.8 μsec as opposed to 0.6 μsec). This point is made clearer by reference to Figure 4 where the vibrational distribution due to electrons

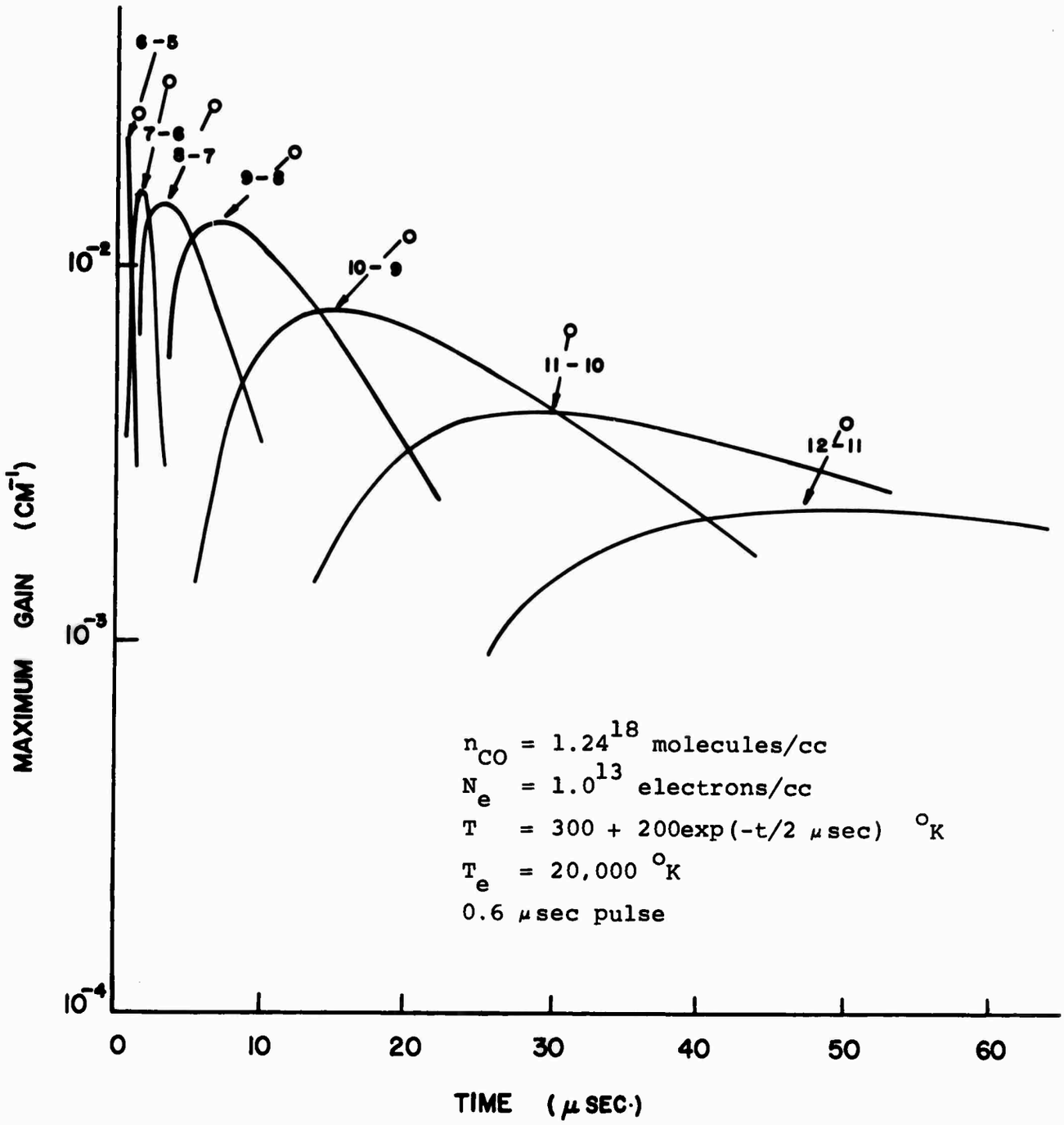

Figure 11: Time sequence of maximum gain for the fundamental transitions in a pulsed CO laser with variable kinetic and rotational temperature. The points refer to "nominal" pulsed CO laser predictions.

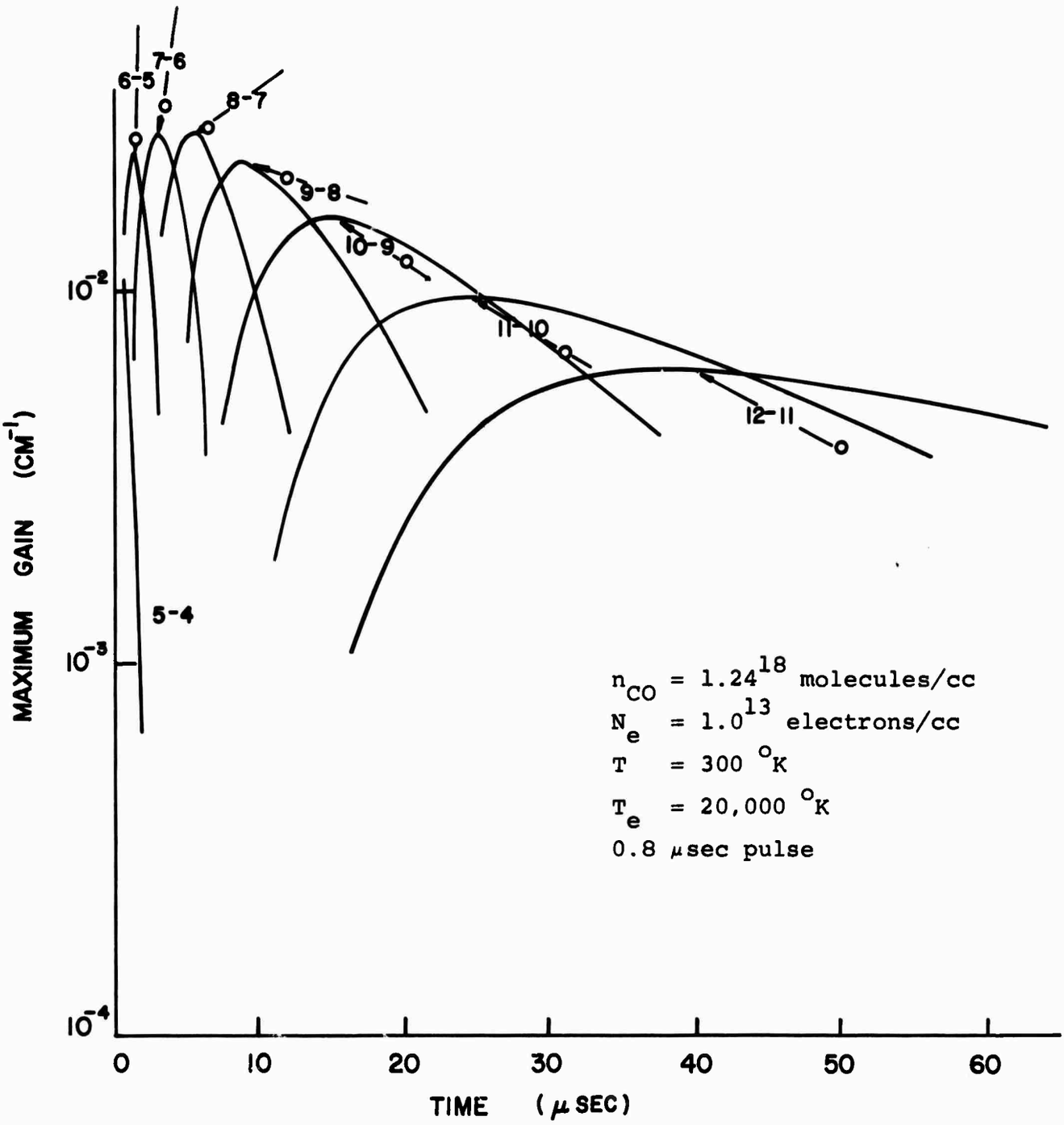

Figure 12: Time sequence of maximum gain for the fundamental transitions in a pulsed CO laser. The points refer to "nominal" pulsed CO laser predictions.

both with and without VV processes is shown for a 0.6 μsec pulse. From this figure it can be noted that the electrons tend to give a smoother vibrational distribution without than with VV processes. Therefore, the distribution due to 0.8 μsec electrons will tend to be smoother on time scales of a few μsec than for only 0.6 μsec pulse widths even though the total energy in the distribution is greater. This latter fact is reflected in the longer time scales of figure 12 (and higher transitions) where the gain is seen to increase over the "nominal" case. Thus, after a time sufficient for the initial distribution to be destroyed, the VV processes rearrange the energy consistant with the ratio of the anharmonicity to kT.

By contrast to this case, we calculated the effect of added N_2 on the pulsed CO laser performance. In a broad sense, since N_2 is an additional sink for electron energy and since N_2 will tend to preferentially pump CO by vibration-vibration exchange processes due to the smaller spacing of CO, we might expect to find increased laser gains by the addition of N_2 to the system. This expectation is not observed as is shown in figures 13 through 15.

The predicted maximum gains are shown in figure 13 for the case in which the N_2 concentration is twice the CO concentration. We note that the delay times are shortened especially for the higher order transitions which the gains are uniformly decreased. The reasons for this behavior are a direct result of the anharmonic character of VV processes. Although N_2 picks up a considerable amount of energy from the electrons during the pulse time, the important point is the mechanism by which N_2 vibrational energy couples to the CO

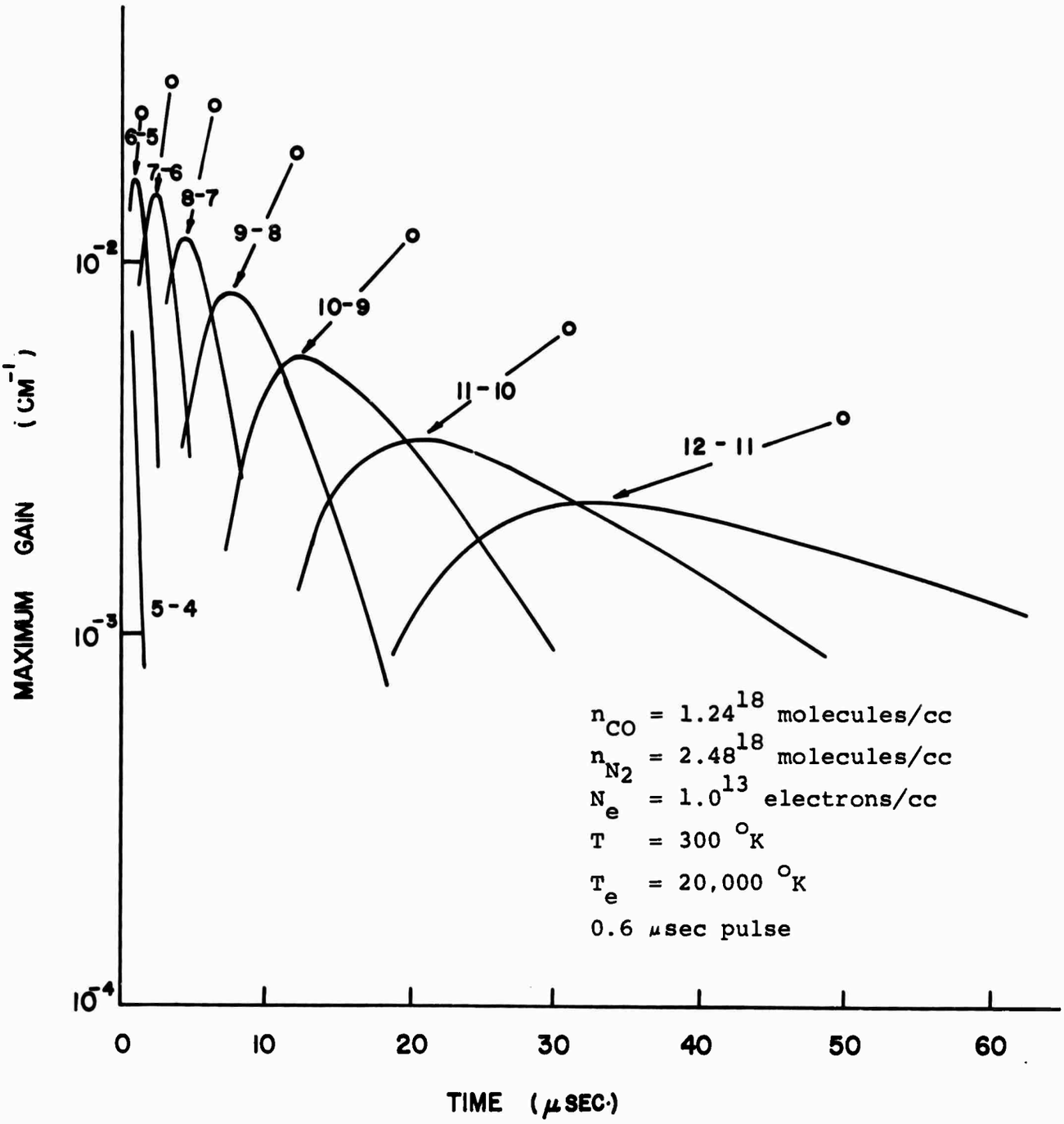

Figure 13: Time sequence of maximum gain for the fundamental transitions in a pulsed CO/N_2 laser. The points refer to "nominal" pulsed CO laser predictions.

vibrational population, i.e. how does vibrational energy flow between N_2 and CO. Due to the layer vibrational spacing of N_2 and the fact that the VV rate coefficients generally increase the closer the resonance in the vibrational quanta being exchanged, vibrational energy from N_2 tends to flow into CO via the low levels where the resonance is closest. Thus, although CO picks up a large amount of energy from N_2 it does this in a way which decreases the inversion between levels and therefore produces decreased gains. However, since the low levels of CO have a layer population than the "nominal" case, VV rates in CO are higher and hence the time delays are shorter.

A further understanding of this N_2-CO transfer can be seen by reference to figures 14 and 15 where the vibrational distribution due to the electrons and subsequent VV relaxation are displayed. Since the VV transfer from N_2 to CO is accompanied by several hundred cm^{-1} anharmonicity, the CO distribution due to hot electrons is essentially identical to that predicted without N_2. However, on longer time scales a comparison of Figure 15 with N_2 to Figure 8 without N_2 shows the greatly reduced inversion with added N_2 and clearly reflects the flow of energy into low levels of CO.

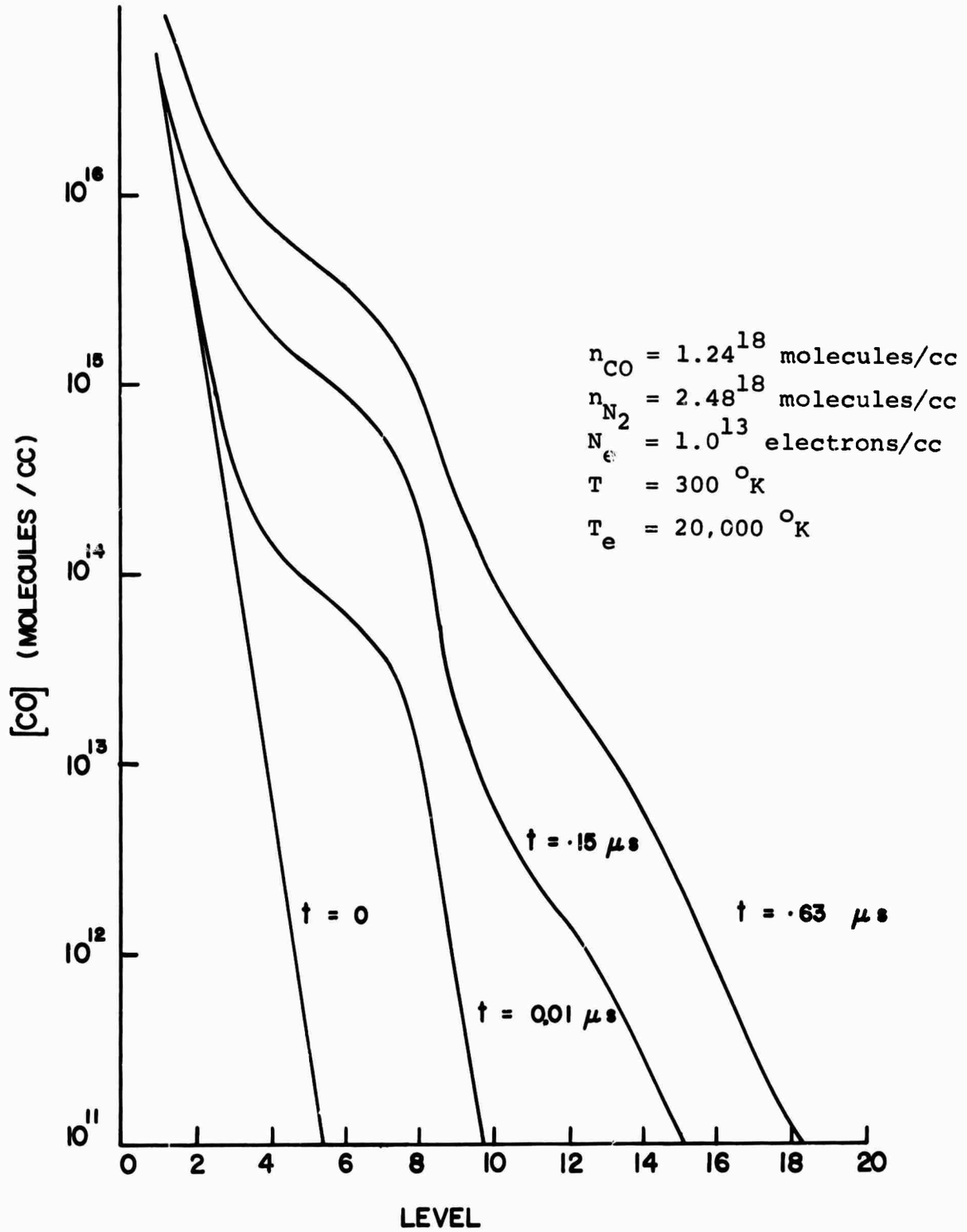

Figure 14: Evolution of the CO vibrational distribution due to hot electrons in a pulsed CO/N_2 laser.

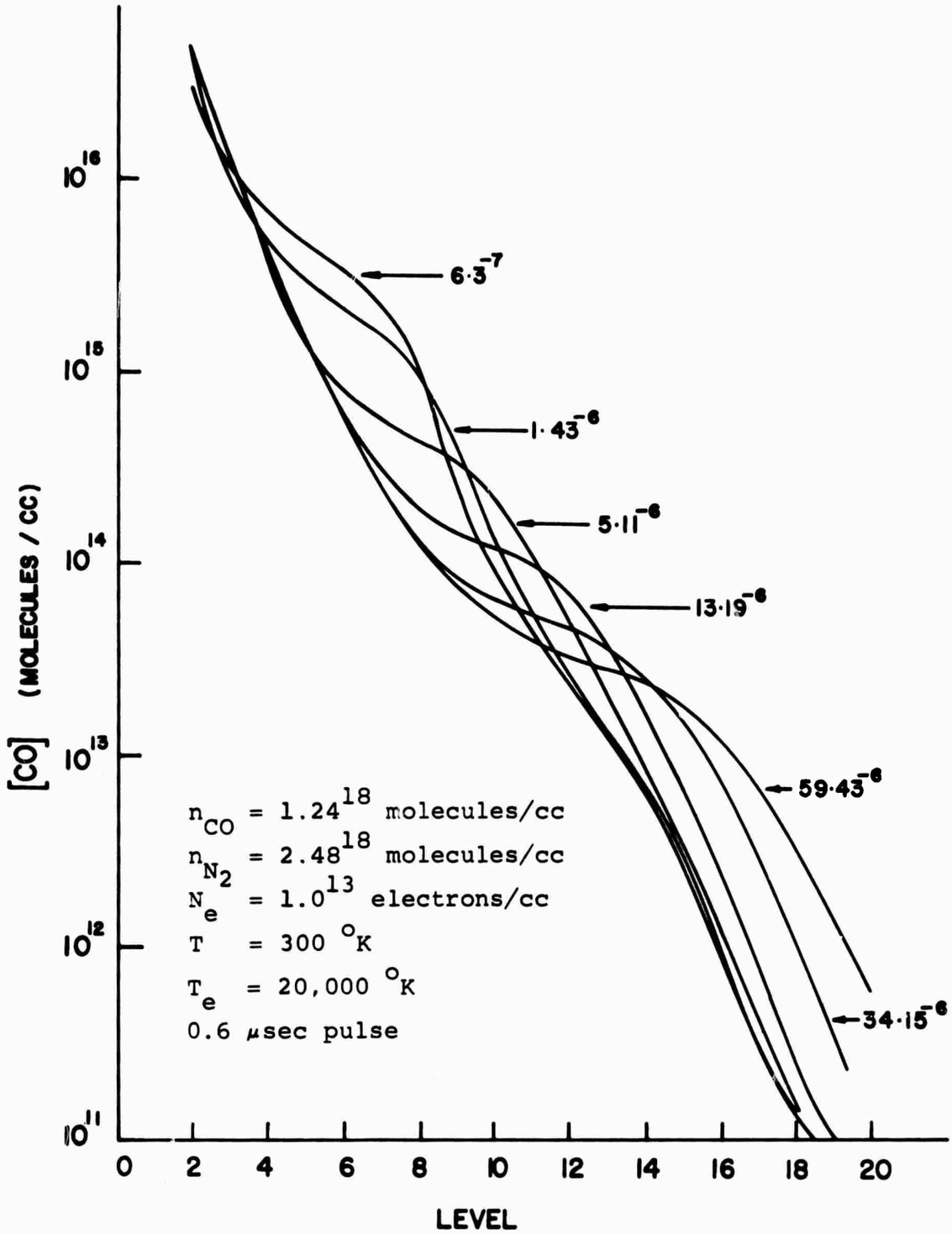

Figure 15: Evolution of the CO vibrational distribution due to VV processes following a 0.6 μsec pulse for a CO/N_2 laser.

Discussion

In the main body of this report we have described a full numerical model for the excitation, relaxation and spontaneous emission of a binary molecular gas mixture. For reasonable assumptions on the system parameters we have shown agreement with the delay times to maximum gain in a pulsed CO laser system. Further we have investigated the sensitivity of these predictions to the several assumed experimental varibles. Clearly before extrapolations of these predictions can be made to other systems, more experimental variables need to be measured to permit less flexibility in the assumptions of the numberical model. The measured CO VV rate coefficients at room temperature were important in the model calculations, however, the temperature dependence of these rates is still uncertain even though it is likely that near resonant exchange is dominated by long range forces which non-resonant processes are controlled by short range processes. Also, the magnitude of low temperature VV exchange processes needs to be determined for other molecular systems, i.e. N_2-CO and N_2-N_2. Although VT processes were not important on the short time scales of interest in these pulsed calculations, the scaling of VT rate coefficients shows great variability depending on the model adopted as has been pointed out before[11]. The modeling of CW laser systems will not be reliably performed until the questions of scaling with vibrational level are resolved.

The general features of the electron coupling rates to CO and N_2 are clearly understood by reference to the unstable negative ion mechanism responsible for the large electron - vibrational cross sections. Thus, the electron couples efficiently to vibrational levels having energy nearly equal to the electron affinity of the unstable ion but rather

unefficiently to levels removed from this energy. This feature of the electron-CO coupling is responsible for the partial inversion on levels around $v = 5$ to $v = 7$ and results in these transitions reaching maximum gain at the earliest time delays.

One point indicated in Jeffer's and Wiswall's experiments was the possibility of an increased translational and rotational temperatures due to the hot electron pulse which would decay to some value above ambient on very short time scales. Although the experimental results appeared to show an increase in the rotational temperature of the lasing transitions to about 750°K with a decay time back to ambient after the electron pulse of 2 μsec, the source of this increase in temperature is uncertain. Preliminary conclusions suggest that direct momentum transfer from the electrons to the neutral gas molecules is insufficient to produce a significant temperature increase. Also, the cross sections for rotational excitation are too small[27] to play a role on the short time scales appropriate to the pulsed operation. The only mechanism which appears important is vibrational excitation accompanied by simultaneous rotational excitation. On the short time scales appropriate to pulsed behavior, VT processes are negligible, however, the simultaneous rotational excitation can be easily degraded into thermal energy. Since spatial gradients in the electrons are expected in Jeffer's and Wiswall's experiments, the heated gas can expand into the unheated regions on time scales characteristic of sound propagation, i.e. μsec, rather than being conducted to the wall which would require considerably longer time scales even under high pressure operation. These points need to be further explored in pulsed CO laser systems although it should be indicated that we were unable to obtain a "reasonable" fit to the experimental delay times upon including a time varying kinetic and rotational temperature in the code.

The addition of N_2 to a pulsed CO laser was seen to reduce the predicted gains even though more electron energy was coupled into the laser system. This fact was interpreted as being due to the anharmonic nature of VV processes. Under current investigation is the behavior of pulsed CO laser systems in which other diatomics are added having a smaller vibrational spacing than CO. By the same reasoning as used in the N_2-CO case, a molecule with a smaller vibrational spacing than CO would cause a preferential drain of vibrational energy from vibrational levels of CO most closely resonant with the lowest levels of the added gas. This process could tend to increase the inversion and subsequently the gains in pulsed operations.

Lastly, it should be pointed out that the electron disturbances present in molecular laser systems are not Maxwellian in shape but are non-Maxwellian in which the energy region of maximum coupling to the diatomic gases is under populated[22]. We have not considered this effect in our calculations due to the fact that the calculated electron-molecule excitation rate coefficients are essentially independent of electron temperature above about 10,000°K. Thus, to first order, we can assume a constant electron-molecule rate coefficient calculated on the basis of a Maxwellian electron distribution. When this is done, the actual electron density assumed may not correspond to that in the experiment due to the under population in the important electron energy range. This effect is likely to produce only a factor of 2 or 3 difference in the assumed electron density in the worst case but should not affect any of the qualitative features indicated by this study.

Bibliography

(1) Bhaumik, M.L., Applied Phys. Letters, 17, 188 (1970).

(2) Rich, J.W., Thompson, H.M., Treanor, C.E. and Daiber, J.W., Applied Phys. Letters, 19, 230 (1971).

(3) Yardley, J.T., J. Mole. Spectroc., 35, 314 (1970).

(4) Jeffers, W.Q. and Wiswall, C.E., J. Quantum Elect., QE-7, 407 (1971).

(5) Schulz, G.J., Phys. Rev., 135, A988 (1964).

(6) Chen, J.C.Y., J. Chem. Phys., 40, 3513 (1964).

(7) Young, L.A. and Eachus, W.J., J. Chem. Phys., 44, 4195 (1966).

(8) Caledonia, G.E. and Center, R.E., J. Chem. Phys., 55, 552 (1971).

(9) Yardley, J.T., App. Optics, 10, 1760 (1971).

(10) Fisher, E.R. and Kummler, R.H., J. Chem. Phys., 49, 1075,1085 (1968).

(11) Glass, A.J., Fisher, E.R., Kummler, R.H. and Marriott, R., Final report on Contract No. DAHC04-70-C-0022, May (1971).

(12) Rapp, D. and Englander-Golden, P., J. Chem. Phys., 40, 573, 3120 (1964).

(13) Kelley, J.D., Proceedings of the 24th Gaseous Electronics Conference, October 5-8, Gainesville, Florida, (1971).

(14) Keneshea, T., AFCRL Research Lab. Report, AFCRL-67-0221, Environmental Paper No. 263, April (1967).

(15) Hancock, G. and Smith, I.W.M., Chem. Phys. Letters, 8, 41 (1971).

(16) Hancock, G. and Smith, I.W.M., Applied Optics, 8, 1827 (1971).

(17) Sharp, T.E. and Rapp, D., J. Chem. Phys., 43, 1233 (1965).

(18) Millikan, R.C. and White D.R., J. Chem. Phys., 39, 3209 (1963).

(19) Herzfeld, K.F. and Litovitz, T.A., "Absorption and Dispersion of Ultrasonic Waves", Academic Press, New York (1959).

(20) Abraham, G. and Fisher, E.R., Research Institute for Engineering Sciences Report 71-31, March (1971).

(21) Erhardt, M. and Willman, K.Z., Phys. Rev., 204, 462 (1967).

(22) Nighan, W.L., United Aircraft Research Lab. Report UAR-K199, October (1971).

(23) Patel, C.K.N., Phys. Rev., 136, A1187 (1964).

(24) Penner, S.S., "Quantitative Molecular Spectroscopy and Gas Emissivities", Addison-Wesley, Reading, Mass. (1959).

(25) Patel, C.K.N., Phys. Rev., 141, 71 (1966).

(26) Graham, W.J., Kershenstein, J., Jenson, J.T. and Kershenstein, K., App. Phys. Letters, 17, 194 (1970).

(27) Singh, Y., J. Phys. B, 3, 1222 (1970).